ACS OMEGA

http://pubs.acs.org/journal/acsodf

Article

Study on Effects of Thermal Resistance and Thermal Buoyancy on Oxygen Flow Patterns during Underground Coal Gasification

Wei Guo, Huan Liu, Zhibing Chang, Di Cao, and Shuqin Liu*

Cite This: *ACS Omega* 2021, 6, 32977−32986

Read Online

ACCESS | Metrics & More | Article Recommendations

ABSTRACT: The controllable growth of the cavity is the basis by which underground coal gasification (UCG) can achieve stable production, and the oxygen flow path and velocity are important factors in determining the expansion rate of the cavity. In this paper, a mathematical model of UCG in horizontal channels was developed, and the effects of multiple factors, including temperature, pressure, flow velocity, and the size of the cavity, on the flow pattern, path, and velocity field distribution of oxygen in the cavity were investigated by using COMSOL Multiphysics software. The results showed that temperature and pressure were the influencing factors of thermal buoyancy. In the established model, oxygen formed a counter-clockwise air vortex at the gas injection port under normal pressure, and the range of the air vortex and the gas flow rate increased with the increase in temperature. In the high-temperature area located in the center of the cavity, the phenomenon of oxygen throttling occurred, and the oxygen flow velocity increased. When the maximum temperature in the cavity was over 850 °C, gas back-mixing occurred at the end of the cavity. Under pressurized conditions, the air vortex at the inlet and back-mixing phenomenon at the outlet disappeared. The flow velocity and the cross-sectional area of the cavity determined the thermal resistance. In the model, the flow velocity was between 0.045 and 0.40 m/s and there were both airflow vortices and back-mixing. In addition, with the expansion of the cavity, back-mixing progressively decreased at the outlet and the airflow vortex changed from counter-clockwise to clockwise.

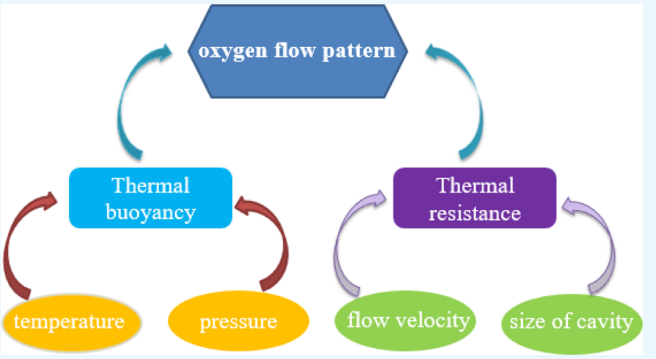

1. INTRODUCTION

Underground coal gasification (UCG), as an in situ chemical conversion and mining technology, can not only be used for the exploitation and utilization of deep and unminable coal seams but can also recover coal resources from abandoned mines. Therefore, it is an important component of the theoretical systems, including green mining, fluidized mining, and precision development of coal resources, and an advantageous supplement to conventional coal mining methods.[1−3] In addition, given significant technical advantages such as good security, low investment, high efficiency, and low pollution, this technology is also deemed to be the focus of harmless coal mining and the strategic direction for technological innovation.[4−6] The UCG transforms physical mining into chemical mining, realizes unmanned underground mining, and avoids the occurrence of mine accidents. Furthermore, it also eliminates the environmental impact above the ground, reduces the fugitive dust from coal mining and transportation, avoids the stacking of gangue, and minimizes the risk of subsidence.[7−9] The process of UCG can be described as shown in Figure 1. First, vertical or directional drilling is carried out from the ground to the coal seam, and the holes are communicated inside the coal seam to form a gasification reaction channel. After that, the coal seam is

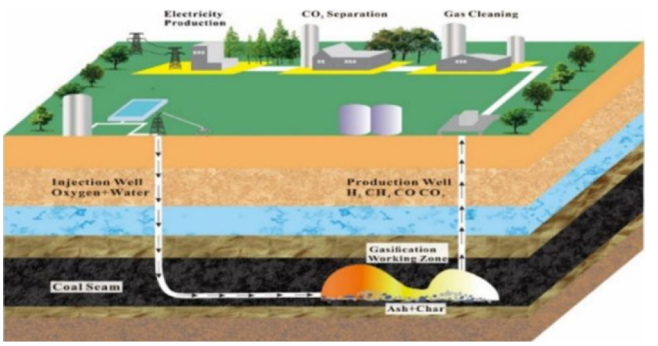

Figure 1. Diagram of the UCG.

Received: September 13, 2021
Accepted: November 15, 2021
Published: November 24, 2021

https://doi.org/10.1021/acsomega.1c05017
ACS Omega 2021, 6, 32977−32986

ignited on one side of the tunnel, and gasification agent is injected from one end of the borehole, including air, oxygen, carbon dioxide, or water vapor. The gasification agent and coal chemically react in the gasification channel to produce an oxidation zone, a reduction zone, and a dry distillation zone. The gasification ash remains underground to generate combustible gas with H_2, CO, and CH_4 as the main components, namely, coal gas. The generated gas is discharged from other boreholes.[10]

As the degree of technology has rapidly increased throughout the 21st century, modern UCG technology (based on horizontal wells of coal seams) and mobile gas injection equipment has become increasingly mature.[10,11] By having a retractable injection of oxygen, cavities can be continuously formed in the coal seam, thus allowing for a continuous production of syngas, which provides the foundations for the expansion of the scale. However, the stability of gas production caused by the expansion of the combustion chamber is still a technical problem for UCG.As one of the important phenomena affecting UCG performance, the expansion of the cavity is the key element in controlling the stability of the UCG process.[12] The cavity is the area created by the gasification process, which consists of a cavity bottom, a roof rock, and a void space between them.[13] At the beginning of the UCG process, an exothermic reaction of coal combustion is usually required to create a sufficiently large underground cavity. Under oxygen injection conditions, the cavity continues to expand and the volume of the central oxygen-free channel constantly increases as the reaction progresses, thus causing poor contact conditions between oxygen and the coal walls. The combustion of flammable gases in the cavity is enhanced, and even the combustion process becomes the dominant reaction, thus resulting in a decrease in the effective components of the outlet gas and degradation in the quality of the gas.[14] In the UCG reaction process, the expansion of the cavity involves the reaction between the gasifying agent and the coal wall.[15] The combustion rate is limited not only by the chemical reaction rate but also by the diffusion rate of oxygen to the channel wall.[16−18] Therefore, in the high-temperature reaction zone, the flow pattern and changing law of oxygen are essential to control the UCG process.

Due to the complexity of the UCG process, there has been an increasing number of studies on the UCG model to improve the UCG reaction system and to make a significant contribution to the development of coal underground gasification. Prabu established a model to demonstrate that the oxygen flow rate has a significant effect on the shape of the cavity. At low flow rates, the reaction is confined to a small area in the cavity, which appears to be spherical. At high flow rates, the oxygen flow rate affects the expansion of the combustion cavity in the axial and radial directions. The shape of the cavity is a typical teardrop shape,[19,20] and the composition of the gasification agent has a little effect on the shape of the cavity.[21] However, the author did not study the specific flow of oxygen in the combustion cavity. Park and Edgar[22] adopted a one-dimensional model to study the development of the early stage of the UCG process. The results indicated that, in the early stage of gasification, the development of the cavity is mainly driven by the oxygen content of the injected gas and the reaction activity of coal itself; later in the UCG process, the gasification properties are the principal contributing factor. However, the model failed to simulate oxygen flow. Perkins et al.[23] simulated the profile of the velocity range in the combustion cavity and studied the influence of well spacing on the gas velocity profile. However, the velocity field of the gas flow in the cavity was not thoroughly investigated. In addition, Bhutto[24] et al. employed the CFD simulation method to evaluate the cavity in combination with the residence time distribution. In this study, the UCG cavity was used as a simplified network of an ideal reactor, and the simulation results reflected the velocity distribution in the cavity. Samdani[13,25] used CFD to simplify the complex combustion cavity to a model consisting of a radial plug flow reactor and a continuous stirred-tank reactor. Despite intensive studies on the nonideal flow pattern in the cavity, the influencing factors of the gas flow pattern remain largely unexplored.

In summary, the mechanism in the previous literature has not yet been studied in great detail, especially for the flow pattern of oxygen under the action of thermal buoyancy and thermal resistance, which has caused the chemical reaction mechanism in the cavity to not be elucidated. Therefore, the purpose of this paper was to develop a mathematical model of UCG in horizontal channels, and the effects of temperature, pressure, flow velocity, and the size of the cavity on the flow pattern path and velocity field distribution of oxygen in the cavity were investigated by using COMSOL Multiphysics commercial software. Consequently, the effects of thermal buoyancy and thermal resistance on oxygen flow characteristics were identified.

2. RESULTS AND DISCUSSION

The flow field in the cavity directly affected the diffusion and distribution of oxygen and determined the chemical reaction rate and the stability of the UCG process. The flow of oxygen in the cavity was primarily influenced by thermal resistance and thermal buoyancy. Thermal buoyancy is a type of thermal convection that is caused by circulating flow from changed fluid pressure or density due to the existence of a nonuniform temperature field.[26] As shown in eq 1, ρ is a function related to P and T, P is the system pressure (Pa), R is the gas constant [8.314 J/(mol*K)], T is the system temperature (K), w_i is the mass concentration of the component i (%), and M_i is the molar mass of the component i (g/mol). Therefore, temperature and pressure play decisive roles in the flow of oxygen. Thermal resistance is a drag of gas flow driven by a pressure drop when the gas passes through the high-temperature zone and when the volume expands.[27] As shown in eq 2, S is the cross-sectional area of the combustion cavity (m^2), φ is the total absorbed heat of gas per unit time and volume in the fire source area [J/(m*s)], and Q is the gas volume flow rate (m^3/s). Moreover, the thermal resistance is related to the gas flow rate and the cross-sectional area of the cavity. To study the influence of thermal resistance and thermal buoyancy, four variables of temperature, pressure, gasification agent flow rate, and the shape and size of the cavity were examined to explore the influence of oxygen flow.

$$\rho_{\mathrm{mix}} = \frac{P}{RT}\sum_i w_i M_i \tag{1}$$

$$h_{\mathrm{a}} = \frac{\varphi Q v_1}{2Sc_{\mathrm{p}}T_1} = \frac{\varphi}{2S^2 c_{\mathrm{p}}T_1}Q^2 \tag{2}$$

2.1. Influence of the Temperature Field on Oxygen Flow. UCG is a self-heating equilibrium process. The temperature field in the gasifier plays an important role in the UCG reaction, which not only affects the chemical reaction rate but also affects the flow of oxygen. Temperature can not only directly change the density of the airflow in the cavity, generate thermal buoyancy, and affect the flow state of the gas but it can

https://doi.org/10.1021/acsomega.1c05017
ACS Omega 2021, 6, 32977−32986

also generate thermal resistance, which causes the appearance of thermal blockages and affects the viscosity resistance coefficient and kinetic energy of the flowing gas.[27] To study the influence of the temperature field on the oxygen flow, four different temperature fields, as shown in Table 1, were set up in the cavity. In the model, the gasification agent flow rate was 0.045 m/s and the ratio of H_2O (g)/O_2 was 2:1.

Table 1. Temperature Field Distribution in the Cavity

	T_{max} (°C)	T_{min} (°C)
A	1250	850
B	1050	650
C	850	450
D	650	250

Figure 2 is a schematic diagram of oxygen flow under different temperature fields in the cavity. Oxygen flows forward into the high-temperature zone, and a counter-clockwise airflow vortex, which is caused by thermal buoyancy and thermal resistance in the high-temperature zone, is formed near the inlet. The higher the temperature, the greater the gas density difference and thermal buoyancy. Additionally, the kinetic energy of the high-temperature gas increases, and the vortex range of the gas flow increases. When the highest temperature is 1250 °C, the flow velocity in the vortex reaches 0.06 m/s. In the middle of the cavity, the gas flows from the high-temperature zone to the low-temperature zone, and the gas volume expands when subjected to heat, thus resulting in decreased pressure and throttling. The cross-section of the cavity is reduced, which increases the flow velocity. The higher the temperature, the more obvious the decrease in pressure and the faster the oxygen flow rate. When the maximum temperature is 1250 °C, the flow velocity reaches 0.06 m/s, and when the maximum temperature is 650 °C, the flow velocity reaches 0.022 m/s. When the maximum temperature is lower than 850 °C, there is no obvious back-mixing phenomenon due to the relatively low temperature and the unobvious influence of the flow field on the airflow. When the maximum temperature is greater than 850 °C, a certain amount of back-mixing occurs due to the large oxygen flow velocity at the end of the cavity. The higher the temperature, the greater the kinetic energy of the gas; additionally, back-mixing is obvious due to the uneven velocity field distribution.

Figure 3 shows the flow flux of oxygen on the surface of the cavity under various temperature field distributions. The higher the temperature, the greater the oxygen flux at the top of the cavity. When the maximum temperature is 1025 °C, the maximum oxygen flux reaches 0.02 mol/(m^2*s). The higher the temperature, the greater the oxygen concentration in the coal wall. In addition, a chemical reaction may cause a violent reaction on the surface and consume a large amount of oxygen. Furthermore, the porosity of the top increases, which causes a large amount of oxygen to contact the wall of the cavity.

2.2. Effect of the Pressure Field on Oxygen Flow. Due to the fact that the UCG reaction is conducted underground, the reaction process is affected by the formation pressure. Perkins[28] found that the greater the pressure in the cavity, the faster the gas reaction rate and the greater the expansion rate. Three variable parameters of reactor pressure, including 1, 3, and 5 MPa, were selected to study the flow of oxygen in the cavity. In the model, the maximum temperature was 1250 °C, the ratio of H_2O (g)/O_2 was 2:1, and the gas flow rate was 0.045 m/s.

According to thermal buoyancy eq 1, the thermal buoyancy is directly proportional to pressure. After the oxygen enters the cavity, it flows to the top of the cavity, which is affected by the inlet pressure, thermal buoyancy, and high-temperature thermal resistance. After the pressure is increased to 1 MPa, the maximum gas flow velocity in the cavity increases by approximately 0.06 m/s for every increase of 1 MPa. In the middle and outlet of the combustion cavity, oxygen also flows to the top of the cavity due to the outlet pressure and pressure difference caused by throttling. Due to the fact that the oxygen level velocity at the outlet is small, there is no back-mixing phenomenon. It can be predicted that if a reaction occurs, a large amount of oxygen will participate in the heterogeneous reaction with coal, thereby increasing the axial expansion rate. The study

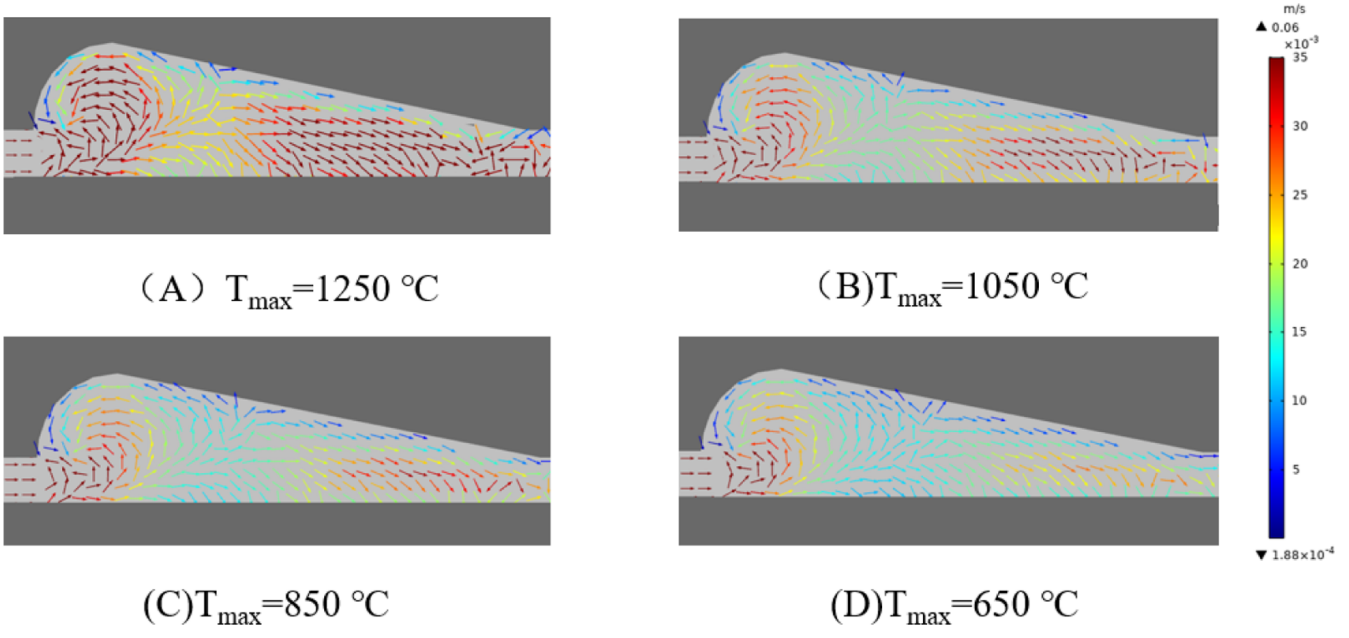

Figure 2. Oxygen flow under different temperature distributions. The maximum temperature is (A) 1250, (B) 1050, (C) 850, and (D) 650 °C.

https://doi.org/10.1021/acsomega.1c05017
ACS Omega 2021, 6, 32977−32986

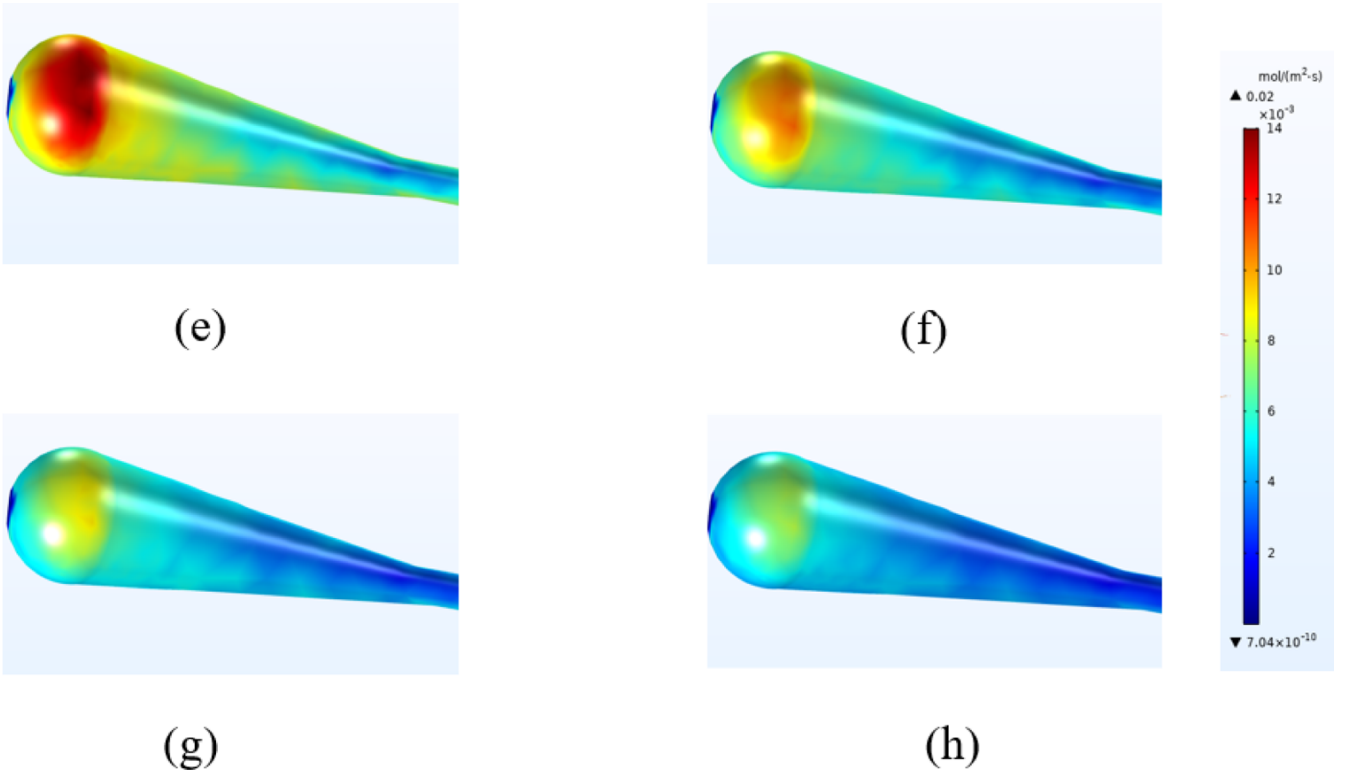

Figure 3. Oxygen flux in the combustion cavity under different temperature distributions. (e−h) Oxygen flux of the combustion cavity under the four conditions of (A−D).

of a zero-dimensional submodel created by Perkins[28] showed that the expansion rate of the fuel cavity increases with increasing pressure. This conclusion is verified from the numerical simulation (Figure 4).

2.3. Effect of the Velocity Field on Oxygen Flow. The study associated with the two-dimensional model of Harloff[29] predicted that the axial expansion rate of the cavity increases monotonically with the gas flow velocity. The increase in gas flow velocity improves the velocity of a large amount of gas flowing into the wall of the cavity, thereby increasing coal consumption and cavity growth.[13] To study the effect of flow velocity on the oxygen flow in the combustion cavity, 10 variable parameters of different flow velocities were selected, including 0.025, 0.030, 0.035, 0.040, 0.045, 0.1, 0.2, 0.3, 0.4, and 0.5 m/s. In the model, the highest temperature was 1250 °C, the ratio of $H_2O(g)/O_2$ was 2:1, and the pressure was normal.

From thermal resistance eq 2, it can be concluded that, at a certain temperature, the thermal resistance is proportional to the square of the flow rate. When the flow velocity is lower than 0.035 m/s, the oxygen flow rate is relatively slow and the thermal resistance is relatively small. The flow field has a little effect on the flow of oxygen; there is no airflow vortex, and the gas slowly fills the combustion cavity. When the flow velocity is greater than 0.035 m/s, the thermal resistance increases to hinder the gas flow. When the flow velocity is between 0.035 and 0.40 m/s, the thermal resistance increases to hinder the gas flow. Under the combined action of thermal buoyancy and thermal resistance, a counter-clockwise airflow vortex is produced and the airflow vortex area increases with increasing inlet flow velocity. A part of the gas flows toward the top of the cavity under the influence of the vortex, and a part flows along the horizontal channel. When the flow velocity is greater than 0.40 m/s and due to the fact that the flow velocity is too large, most of the gas flows out along the horizontal channel and the gas flow vortex disappears. In the middle of the combustion cavity, the gas flow velocity becomes larger due to throttling. When the flow velocity is between 0.035 and 0.40 m/s, the back-mixing phenomenon occurs at the end of the cavity. The greater the air inlet flow velocity, the more obvious the back-mixing. When the flow velocity is greater than 0.40 m/s, the oxygen that flows to the top of the cavity decreases and the back-mixing gradually disappears. The airflow vortex can promote the reaction of oxygen with the wall of the combustion cavity, and the backflow can make the oxygen more fully react with the gas in the cavity to produce high-quality coal gas components. Therefore, the most ideal flow velocity range is 0.045−0.40 m/s (Figure 5).

2.4. Influence of Cavity Geometry on Oxygen Flow. The expansion of the cavity in all directions gradually increases with the operating time. According to studies by Daggupati[15] and Jowkar,[30] the parameters at different operating times are selected, and the expansion length in every direction is shown in Figure 6 and Table 2.

According to the thermal resistance eq 2, it can be concluded that the cross-sectional area of the cavity and the thermal resistance are inversely proportional when other conditions are unchanged. Although the thermal resistance becomes larger, no back-mixing occurs at the outlet of the cavity. This is mainly attributed to the small cross-sectional area of the combustion cavity in the gas injection pipe as well as the fast gas flow rate and the counter-clockwise flow of the gas along with the vortex. When the cavity gradually increases, the gas still flows counter-clockwise along with the vortex, with the airflow at the outlet being chaotic and back-mixing occurring. When the cavity continues to increase, the cross-sectional area of the gas injection port cavity becomes larger, the oxygen horizontal flow rate slows down, and the oxygen moves to the top of the cavity under the

https://doi.org/10.1021/acsomega.1c05017
ACS Omega 2021, 6, 32977−32986

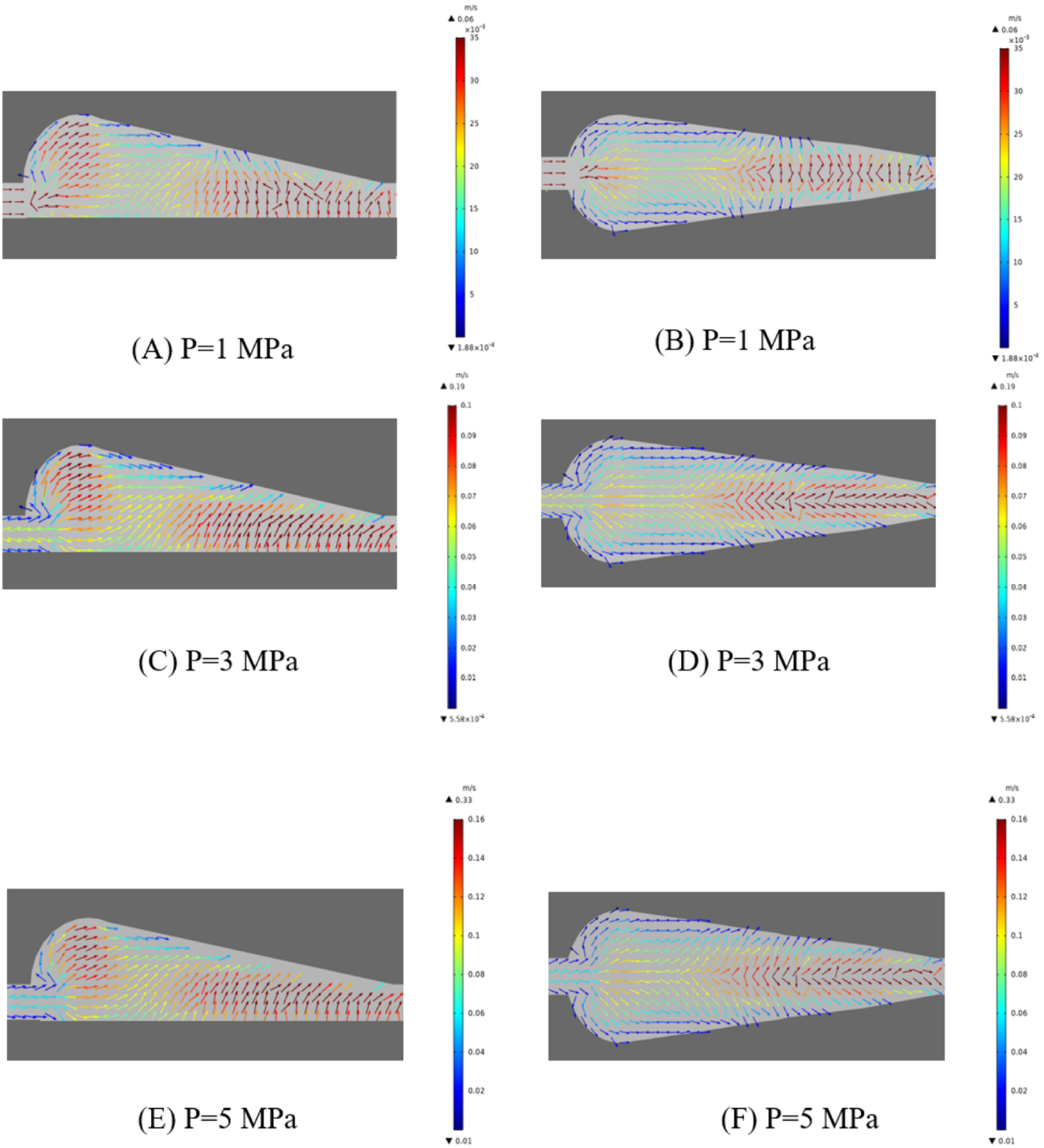

Figure 4. Oxygen flow under different pressures. (A,C,E) Front views of oxygen flow under various pressures and (B,D,F) vertical views of oxygen flow under various pressures.

influence of thermal buoyancy and thermal resistance. The gas in the airflow vortex changes from counter-clockwise to clockwise, and the phenomenon of back-mixing at the outlet is more obvious.

3. CONCLUSIONS

This paper developed a mathematical model of underground gasification in a horizontal channel and explored the influence of the temperature field distribution, pressure, gasification agent flow velocity, and cavity size on the flow of oxygen in the cavity.

1. When oxygen enters the combustion cavity, a counter-clockwise flow vortex is formed near the air inlet. The higher the temperature, the larger the airflow vortex area and the faster the oxygen flow velocity. In the middle of the cavity, a throttling phenomenon occurs due to the thermal expansion of airflow volume, thereby causing the flow velocity to increase. In addition, a certain amount of

https://doi.org/10.1021/acsomega.1c05017
ACS Omega 2021, 6, 32977−32986

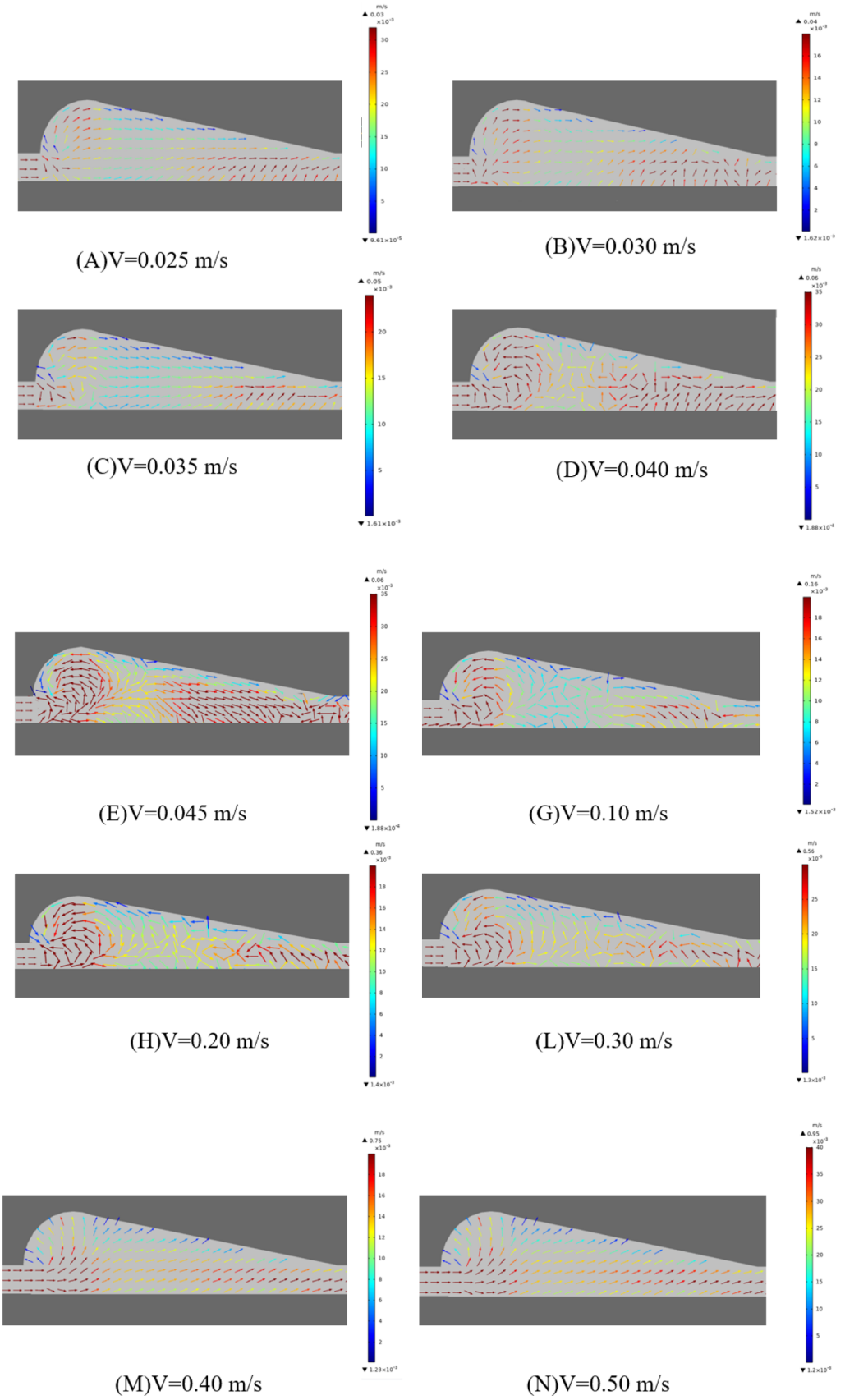

Figure 5. Oxygen flow at different flow velocity. (A).0.025 m/s (B).0.030 m/s (C).0.035 m/s (D).0.040 m/s (E).0.045 m/s (G).0.10 m/s (H).0.20 m/s (L).0.30 m/s (M).0.40 m/s (N).0.50 m/s.

https://doi.org/10.1021/acsomega.1c05017
ACS Omega 2021, 6, 32977−32986

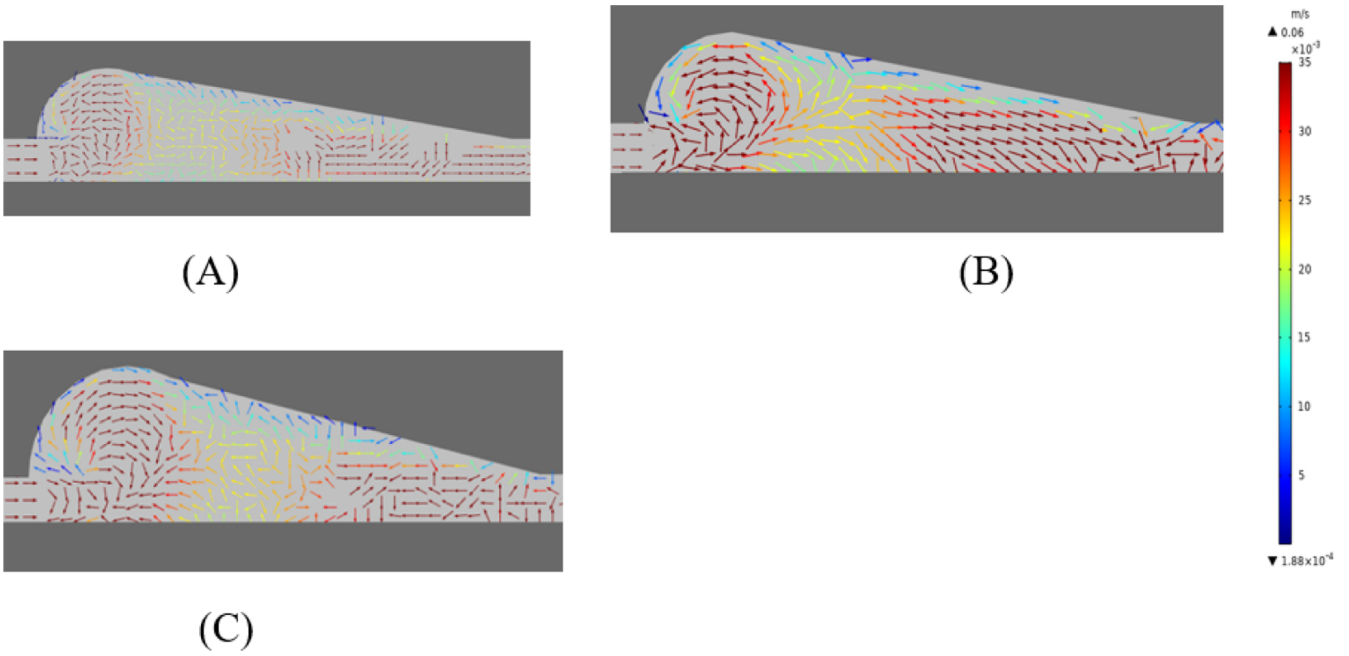

Figure 6. Oxygen flow in different cavity sizes. (A−C) Oxygen flow in the three different cavity sizes in Table 2.

Table 2. Expansion of the Fuel Cavity in All Directions

	B (cm)	F (cm)	H (cm)	L (cm)	W (cm)
A	0.5	7.4	1.6	0.67	1.2
B	1.15	8.86	1.8	0.8	1.5
C	1.3	9.6	2.2	1.08	1.8

back-mixing appears at the end of the cavity when the maximum temperature is above 850 °C; the higher the temperature, the more pronounced the back-mixing.

2. Under pressurized conditions, the air vortex near the air inlet disappears. After the pressure is increased to 1 MPa, the maximum gas flow velocity in the cavity increases by 0.06 m/s for every 1 MPa of increased pressure. In the middle and rear parts of the combustion cavity, most of the oxygen flows to contact the wall of the cavity. The oxygen level velocity at the outlet is relatively small, and no back-mixing will occur.
3. When the flow velocity is between 0.035 and 0.40 m/s, a counter-clockwise air vortex is generated; the greater the inlet rate i, the larger the air vortex area. When the flow velocity is between 0.045 and 0.40 m/s, the back-mixing phenomenon occurs at the outlet of the cavity. For the cavity, the optimal flow velocity is 0.045−0.40 m/s.
4. The oxygen flows counter-clockwise along with the vortex when the size of the cavity is relatively small, and there is no back-mixing phenomenon at the outlet. As the cavity increases in size, oxygen still flows counter-clockwise along the vortex, whereas back-mixing gradually occurs at the outlet. When the cavity continues to increase, the cross-sectional area becomes larger, the oxygen vortex flow changes from counter-clockwise to clockwise, and the back-mixing phenomenon at the outlet becomes noticeable.

4. MATHEMATICAL MODEL ESTABLISHMENT

UCG is an extremely complex process because it encompasses different disciplines, ranging from flow to heat and mass transfer.

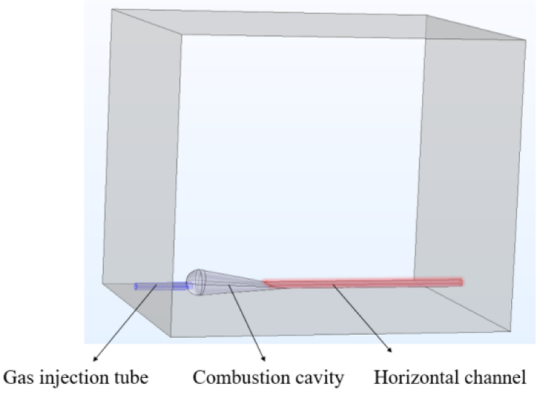

Figure 7. Mathematical model of underground gasification in horizontal coal seam channels.

This study simulated the UCG process of horizontal channels. In terms of the numerical simulation of the oxygen flow in the cavity, the urgent issues that needed to be addressed included the coupling interactions among gas seepage flow, the temperature conduction and convection, and the coal seam pressure field. Given the complexity of the UCG process, the following assumptions were made to study the flow of oxygen in the cavity.

(1) Coal is homogeneous and isotropic. The joints and faults in coal are ignored. The diffusivity and thermal conductivity in different directions are identical, and the cavity is horizontally symmetrical.
(2) Accidental circumstances, such as the collapse of the coal seam and the impact of the generated ash on the model, are negligible.
(3) Only diffusion and convection are considered in the model, and the influence of heat radiation in the cavity is ignored.

4.1. Governing Equation. After creating a reasonable physical model in COMSOL software, the first step is selecting

https://doi.org/10.1021/acsomega.1c05017
ACS Omega 2021, 6, 32977−32986

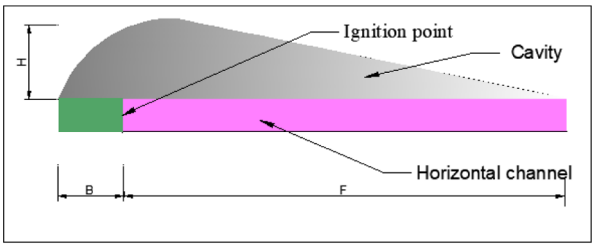

(A) Front view

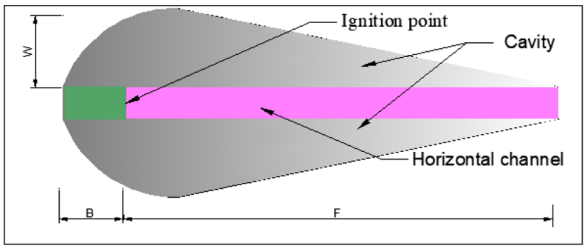

(B) Vertical view

Figure 8. Plan and top view of the cavity.

Table 3. Expansion of the Fuel Cavity in All Directions

B (cm)	F (cm)	H (cm)	W (cm)
1.15	8.86	1.8	1.5

appropriate equations from the model of COMSOL to address flow, pressure, and heat transfer. Then, the equations are added, subtracted, and optimized according to the characteristics and parameters tightly related to UCG, and control eqs 3−8 are obtained.

(1) pressure field-governing equation. For UCG, the flow phenomenon is more complicated. Although most of the cavity is a laminar flow zone, the Reynolds number is relatively large near the gas injection point and high-temperature zone, and the gas flow state is turbulent.[31,32] Darcy's law is generally used to simulate the flow in the laminar flow zone and is not applicable for simulating the airflow in the cavity. To simulate the real gas-phase motion and to consider the influence of dynamic viscosity on the turbulence phenomenon, the Brinkman equation was adopted in this paper, and the fluid was assumed to be incompressible:

$$\rho\frac{\partial u}{\partial t} = \nabla\cdot[-p^2 + K] + F + \rho g \tag{3}$$

$$\frac{\partial \rho}{\partial t} + \nabla\cdot(\rho u) = 0 \tag{4}$$

$$K = \mu(\nabla u + (\nabla u)^T) - \frac{2}{3}\mu(\nabla\cdot u) \tag{5}$$

where F is the stress source term, u is the gas flow velocity, m/s, μ is the dynamic viscosity, kg/m·s, and ρ is the density of the mixed gas, kg/m^3.

(2) concentration field control equation. The gas flows in the cavity and horizontal channel and the flow path and velocity are affected by the concentration difference and thermal buoyancy, thus forming a certain concentration field.

$$\frac{\partial c_i}{\partial t} + \nabla\cdot J_i + u\cdot\nabla c_i = R_i \qquad i = O_2 \tag{6}$$

$$J_i = -D_i\nabla c_i \tag{7}$$

where c_i is the concentration of the component i, mol/m^3; D_i is the diffusion coefficient of the component i, mol/m^2; and R_i is the source term of the generation or reaction of the component i, mol/m^3.

(3) temperature field control equation. The heat transfer mechanism has three basic forms: heat conduction, convection heat transfer, and heat radiation.[33] Among them, the transmission of heat achieves heat transfer through fluid flow, whereas thermal radiation realizes heat transfer due to the object's temperature emission of visible

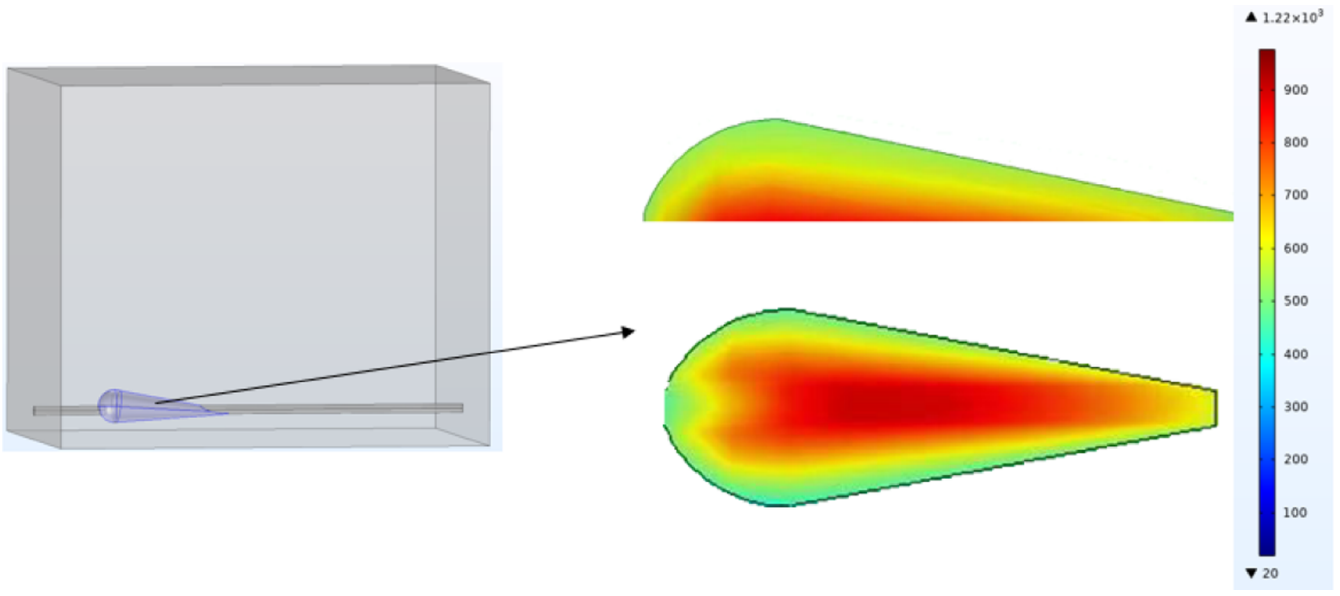

Figure 9. Temperature field distribution of the cavity.

https://doi.org/10.1021/acsomega.1c05017
ACS Omega 2021, 6, 32977−32986

Table 4. Proximate Analysis and Ultimate Analysis of Coal

proximate analysis		ultimate analysis					
volatile matter %	fixed carbon %	moisture %	ash %	carbon %	hydrogen %	nitrogen %	oxygen %
37.18	58.58	16.91	5.61	59.47	3.08	0.99	13.79

or invisible rays. In the UCG process, coal is continuously burned and consumed, thus forming a cavity in the coal seam. The gas flows in the combustion zone by means of heat conduction and convective heat transfer and radiation heat transfer is negligible.[34] Because the reaction process is a self-heating process and most of the thermal radiation energy is absorbed by the gas in the cavity, the temperature difference in the combustion area is not large. The equations for heat conduction and convective heat transfer are eq 8, in which, the second term in the equation contains u_g, which is a term related to speed, and its value is larger than the value of thermal radiation. Therefore, in order to simplify the calculation, the radiation heat transfer is ignored in the model. Assuming isotropy, the internal heat source in the temperature field of the coal seam is the heat derived from the combustion of coal or gas, and the temperature field control equation of the coal seam is shown in eq 8.

$$(\rho C_p)_{cq}\frac{\partial T}{\partial t} + \rho C_p u_g \nabla T = \nabla\cdot(k_{cq}\nabla T) + Q \quad (8)$$

where k_{cq} is the equivalent thermal conductivity; $(\rho C_p)_{cq}$ is the equivalent volumetric heat capacity at normal pressure; ρ is the gas density, kg/m^3;C_p is the specific heat capacity of the gas, J/(kg·K); T is the temperature, K; t is the time, s; u_g is the gas velocity, m/s; and Q is the gas heat source sink.

4.2. Model Establishment. *4.2.1. Geometric Model.* A mathematical model of underground gasification in horizontal coal seam channels was established. Because the field test scale is too large to be suitable for simulation, according to similar principles, the gasifier is scaled down to one of the experimental facility to focus on oxygen flow research. Thermal resistance and thermal buoyancy exist whether the UCG scale is large or small. As shown in Figure 7, the coal size was 300 × 250 × 250 mm, the diameter of the gas injection pipe and the horizontal channel was 12 mm, the gas injection pipe length was 50 mm, and the horizontal channel length was 250 mm. Coal is burned, and a cavity is formed during the UCG process.

4.2.2. Cavity Model Establishment. In the UCG process, the intensity of the flame in the vertical direction is approximately twice that in the horizontal direction,[35] which causes the coal seam at the top of the flame upon warming to fall into the horizontal channel due to the rapid development of cracks. The high reaction activity of fresh coal seams that are exposed to the horizontal channel increases the combustion intensity of coal seams and makes the cavity "pear-shaped". A schematic diagram of the cavity is plotted in Figure 8. The expansion length in every direction is represented by B, F, H, and W. The gasification agent that was used in this study is oxygen and steam at a ratio of 1:2. According to Daggupati[15] and Jowkar,[30] the expansion parameters of the cavity are selected as shown in Table 3.

4.2.3. Temperature Field Model Establishment. After oxygen flows into the horizontal channel in the UCG process, a portion of it flows radially and contacts the coal wall to take place in the heterogeneous reaction and to release heat, accompanied by the production of CO, H_2, CH_4, and other gases. The other part of the oxygen diffuses along the horizontal channel and reacts homogeneously with the generated gas. The temperature at the front end of the ignition port is the highest, whereas the temperature on the wall of the cavity is relatively low. Seifi et al.[36] and other studies found that the temperature at the front end of the gas injection pipe in the cavity is the highest, which can be up to 1250 °C. Additionally, the temperature of the coal wall is approximately 850 °C. The temperature is uniformly reduced to the outside to simplify the temperature field. The front and top views along the horizontal channel are shown in Figure 9.

4.2.4. Proximate Analysis and Ultimate Analysis of the Target Coal Sample. The simulated coal samples came from the Baolige coal fields in the Xilin Gol League of Inner Mongolia in China. Borehole sampling was used, and the sampling depth was approximately 671.71−683.17 m. The proximate analysis and ultimate analysis of coal are shown in Table 4.

4.2.5. Boundary Conditions.

(1). Pressure field boundary conditions

inlet boundary conditions $u\cdot n = u_0$

outlet boundary conditions $p = p_0$

other boundary conditions are nonslip boundaries $u = 0$

(2). Concentration field boundary conditions

$c_i = c_{i,0}$

When assuming that the gas is mainly controlled by convection mass transfer, the diffusion flux at the outlet of the gasifier is c.

$$n\cdot(-D_i\nabla c_i) = c$$

The outlet boundary conditions are

$$N_i\cdot n = c_i u\cdot n$$

When assuming that there is no mass transfer between the gasifier wall and the outside during the gasification process, the boundary condition of the coal seam is

$$N_i\cdot n = 0$$

AUTHOR INFORMATION

Corresponding Author

Shuqin Liu − *School of Chemical and Environmental Engineering, China University of Mining and Technology, Beijing 100083, P.R. China;* orcid.org/0000-0002-7670-7999; Email: liushuqin@cumtb.edu.cn

Authors

Wei Guo − *School of Chemical and Environmental Engineering, China University of Mining and Technology, Beijing 100083, P.R. China*

Huan Liu − *School of Chemical and Environmental Engineering, China University of Mining and Technology, Beijing 100083, P.R. China*

Zhibing Chang − *School of Chemical and Environmental Engineering, China University of Mining and Technology,*

https://doi.org/10.1021/acsomega.1c05017
ACS Omega 2021, 6, 32977−32986

Beijing 100083, P.R. China; orcid.org/0000-0002-3339-0020

Di Cao − *School of Chemical and Environmental Engineering, China University of Mining and Technology, Beijing 100083, P.R. China*

Complete contact information is available at: https://pubs.acs.org/10.1021/acsomega.1c05017

Notes

The authors declare no competing financial interest.

■ ACKNOWLEDGMENTS

This research was supported by the Natural Science Foundation of China (project number 51476185), the Beijing Collaborative Innovation Project of Applied Technology in the Field of Energy and Materials (project number Z201100004520012), and the China University of Mining and Technology (Beijing) Yueqi Outstanding Scholar Project (project number 2020JCB02).

■ REFERENCES

(1) Qian, M. G.; Xu, J. L.; Miu, X. X. Green technique in coal mining. *J. China Univ. Min. Technol.* **2003**, *32*, 343−348.
(2) Xie, H.; Gao, F.; Ju, Y.; Ge, S. R.; Wang, G. F.; Zhang, R. Theoretical and technological conception of the fluidization mining for deep coal resources. *J. China Coal Soc.* **2017**, *42*, 547−556.
(3) Yuan, L.; Jiang, Y. D.; Wang, K.; Zhao, Y. X.; Hao, X. J.; Xu, C. Precision exploitation and utilization of closed/abandoned mine resources in China. *J. China Coal Soc.* **2018**, *43*, 14−20.
(4) Gregg, D. W.; Edgar, T. F. Underground coal gasification. *Chem. Eng. Prog.* **2012**, *24*, 1036.
(5) Samdani, G.; Aghalayam, P.; Ganesh, A.; Mahajani, S. A process model for underground coal gasification − Part-III: Parametric studies and UCG process performance. *Fuel* **2018**, *234*, 392−405.
(6) Yuan, L. Strategic thinking of simultaneous exploitation of coal and gas in deep mining. *J. China Coal Soc.* **2016**, *41*, 1−6.
(7) Yang, L. Three-Dimensional unstable non-linear numerical analysis of the underground coal gasification with free channel. *Energy Sources, Part A* **2006**, *28*, 1519−1531.
(8) Ma, W.; Li, Z.; Lv, J.; Yang, L.; Liu, S. Environmental evaluation study of toxic elements (F, Zn, Be, Ni, Ba, U) in the underground coal gasification (UCG) residuals. *J. Clean. Prod.* **2021**, *297*, 126565.
(9) Feng, Y.; Yang, B.; Hou, Y.; Duan, T.-H.; Yang, L.; Wang, Y. Comparative environmental benefits of power generation from underground and surface coal gasification with carbon capture and storage. *J. Clean. Prod.* **2021**, *310*, 127383.
(10) Liu, S. Q.; Shi, S. Z.; Feng, G. X.; Feng, J.; Li, M. X.; Guo, W. Geological site selection and evaluation for underground coal gasification. *J. China Coal Soc.* **2019**, *44*, 2531−2538.
(11) Akbarzadeh Kasani, H.; Chalaturnyk, R. J. Coupled reservoir and geomechanical simulation for a deep underground coal gasification project. *J. Nat. Gas Sci. Eng.* **2017**, *37*, 487−501.
(12) Daggupati, S.; Mandapati, R. N.; Mahajani, S. M.; Ganesh, A.; Mathur, D. K.; Sharma, R. K.; Aghalayam, P. Laboratory studies on combustion cavity growth in lignite coal blocks in the context of underground coal gasification. *Energy* **2010**, *35*, 2374−2386.
(13) Samdani, G.; Aghalayam, P.; Ganesh, A.; Sapru, R. K.; Lohar, B. L.; Mahajani, S. A process model for underground coal gasification − Part-I Cavity growth. *Fuel* **2016**, *181*, 690−703.
(14) Liu, S. Q.; Mei, X.; GUO, W.; Cao, D. Progress of underground coal gasification theory and technology. *Coal Sci. Technol.* **2020**, *48*, 90−99.
(15) Daggupati, S.; Mandapati, R. N.; Mahajani, S. M.; Ganesh, A.; Sapru, R. K.; Sharma, R. K.; Aghalayam, P. Laboratory studies on cavity growth and product gas composition in the context of underground coal gasification. *Energy* **2011**, *36*, 1776−1784.
(16) Perkins, G.; Sahajwalla, V. A mathematical model for the chemical reaction of a semi-infinite block of coal in underground coal gasification. *Energy Fuels* **2005**, *19*, 1679−1692.
(17) Nourozieh, H.; Kariznovi, M.; Chen, Z.; Abedi, J. Simulation study of underground coal gasification in Alberta reservoirs: geological structure and process modeling. *Energy Fuels* **2010**, *24*, 3540−3550.
(18) Perkins, G.; Sahajwalla, V. Steady-state model for estimating gas production from underground coal gasification. *Energy Fuels* **2008**, *22*, 3902−3914.
(19) Prabu, V.; Jayanti, S. Heat-affected zone analysis of high ash coals during ex situ experimental simulation of underground coal gasification. *Fuel* **2014**, *123*, 167−174.
(20) Prabu, V.; Jayanti, S. Simulation of cavity formation in underground coal gasification using borehole combustion experiments. *Energy* **2011**, *36*, 5854−5864.
(21) Prabu, V.; Jayanti, S. Laboratory scale studies on simulated underground coal gasification of high ash coals for carbon-neutral power generation. *Energy* **2012**, *46*, 351−358.
(22) Park, K. Y.; Edgar, T. F. Modeling of early cavity growth for underground coal gasification. *Ind. Eng. Chem. Res.* **1987**, *26*, 237−246.
(23) Perkins, G.; Sahajwalla, V. A numerical study of the effects of operating conditions and coal properties on cavity growth in underground coal gasification. *Energy Fuels* **2006**, *20*, 596−608.
(24) Bhutto, A. W.; Bazmi, A. A.; Zahedi, G. Underground coal gasification: From fundamentals to applications. *Prog. Energy Combust. Sci.* **2013**, *39*, 189−214.
(25) Samdani, G.; Aghalayam, P.; Ganesh, A.; Sapru, R. K.; Lohar, B. L.; Mahajani, S. A process model for underground coal gasification − Part-II Growth of outflow channel. *Fuel* **2016**, *181*, 587−599.
(26) Sheng, D.-Y.; Jönsson, P. G. Effect of Thermal Buoyancy on Fluid Flow and Residence-Time Distribution in a Single-Strand Tundish. *Materials* **2021**, *14*, 1906.
(27) Yang, Z.; Wu, B.; Zhao, A. J.; Huang, J. X.; Li, Y. Numerical simulation study on fire resistance and thermal roundabout flow phenomenon of the tunnel fire. *Int. J. Earth Sci. Eng.* **2016**, *9*, 2577−2582.
(28) Perkins, G. A 0-dimensional cavity growth submodel for use in reactor models of underground coal gasification. *Int. J. Coal Sci. Technol.* **2019**, *6*, 334−353.
(29) Harloff, G. J. Underground coal gasification cavity growth model. *J. Energy* **1983**, *7*, 410−415.
(30) Jowkar, A.; Sereshki, F.; Najafi, M. A new model for evaluation of cavity shape and volume during Underground Coal Gasification process. *Energy* **2018**, *148*, 756−765.
(31) Daggupati, S.; Mandapati, R. N.; Mahajani, S. M.; Ganesh, A.; Pal, A. K.; Sharma, R. K.; Aghalayam, P. Compartment modeling for flow characterization of underground coal gasification cavity. *Ind. Eng. Chem. Res.* **2010**, *50*, 277−290.
(32) Sarraf Shirazi, A.; Karimipour, S.; Gupta, R. Numerical simulation and evaluation of cavity growth in in situ coal gasification. *Ind. Eng. Chem. Res.* **2013**, *52*, 11712−11722.
(33) Zhang, J.; Wang, Z. W.; Song, Z. X. Numerical study on movement of dynamic strata in combined open-pit and underground mining based on similar material simulation experiment. *Arabian J. Geosci.* **2020**, *13*, 43−44.
(34) Wang, Z.; Liang, J.; Shi, L.; Xi, J.; Li, S.; Cui, Y. Expansion of three reaction zones during underground coal gasification with free and percolation channels. *Fuel* **2017**, *190*, 435−443.
(35) Huang, W.-g.; Wang, Z.-t. Mechanical performance evolution and size determination of strip coal pillars with an account of thermo-mechanical coupling in underground coal gasification. *Int. J. Rock Mech. Min.* **2021**, *142*, 104755.
(36) Seifi, M.; Chen, Z.; Abedi, J. Numerical simulation of underground coal gasification using the CRIP method. *Can. J. Chem. Eng.* **2011**, *89*, 1528−1535.